MICROPILE BEARING PLATES: ARE THEY NECESSARY?

Peter Sheffield[1], Xian-Xing Li[2], and Daniela Ramirez[3]

ABSTRACT

This paper presents experimental and analytical results of a full scale micropile cap test carried out to failure. The failure load on the micropile cap reached *2.33* times the design working load, confirming a bearing plate is not necessary in this particular application. The analytical results, consisting of a Finite Element Analysis using fracture mechanics, are in good agreement with the experimental results. The crack patterns, reinforcement stress, and ultimate bearing strength estimated correlate well with the actual results. Recommendations for the design of micropile caps to achieve satisfactory structural performance are provided.

INTRODUCTION

Pile caps transfer loads from superstructures to pile groups beneath. Design procedures for pile caps under compression generally require satisfying four distinct criteria: bearing strength, bending strength, shear strength, and geometric requirements for the embedment of reinforcement. This paper will focus on the bearing strength. The use of plates in pile caps is often required to satisfy the bearing capacity in the concrete above the piles. The plate connection to the micropile is often problematic to construct since it is difficult to ensure there is good contact of grout and the plate inside the casing of the micropile. Bearing plates result in difficulties achieving sound concrete placement beneath the plates and may produce adverse cracking around the steel plates (debonding due to the incompatible deformation), which may damage the integrity of the cap. Large bearing plates also significantly extend or offset the bearing region towards the pile cap edges, which may, in turn, reduce the concrete bearing capacity due to lesser concrete confinement. In the Ohio Highway Department tests (1947), some tests had worse results with a steel bearing plate as opposed to those without bearing plate, indicating a weakening of the pile cap capacity because of the bearing plates. It was hence important to investigate if the use of plates was necessary in this application.

Pile caps are design on the tie and strut method that assumes a straight strut from the column above the cap to each of the piles and a tension tie between the piles. This method is used in the Canadian Concrete Design Handbook. Usually the reinforcement is to be provided in the form of ties spanning from pile to pile as shown in each pile cap table.

---

1. Peter Sheffield P.Eng. Peter Sheffield and Associates, Toronto, Ontario, Canada. psheff@netcom.ca
2. Xian-Xing Li, Ph.D. Peter Sheffield and Associates. Toronto, Ontario, Canada. nnnewww@yahoo.com
3. Daniela Ramirez, P.Eng. Isherwood Associates. Mississauga, Canada. daniela@isherwood.to

HISTORY OF BEARING CAPACITY IN CONCRETE

The ultimate bearing strength of plain and reinforced concrete blocks under concentric loading has been investigated for more than 100 years. The variables influencing the bearing strength of concrete are: concrete strength, geometry of loaded and supported areas, and confining reinforcement. A summary of recent tests correlating bearing and concrete strength, loaded areas will show that concrete bearing strength specified by existing codes may be conservative.

Komendant (1952) proposed a square root formula to account for the effect of the ratio of specimen gross area (often the column area above) A_2, to the loaded area (the pile area), A_1 on the bearing strength. This formula is still being used in many design codes with some modifications. Niyogi (1973), however, conducted experiments on the bearing strength of concrete using different shapes and sizes of bearing plates. He concluded that the ratio of the bearing strength over the concrete compression strength, f_b / f'_c, is not proportional to the square root of A_2 / A_1. Hawkins (1968) found the ratio of the bearing strength over the concrete compressive strength, f_b / f'_c, decreases as f'_c increases. This phenomenon was verified by the experiments carried out by Niyogi (1974) as well as Adebar and Zhou (1993).

In the ACI and Canadian Concrete Design Code current design practice, the bearing strength of concrete is limited to 1.7 times the strength of concrete ($f_b \leq 1.7\, f'_c$). However experiments conducted by Hawkings (1968) and Niyogi (1974) the bearing strength ratio, f_b / f'_c, is more than 1.7 for large ratios of A_2 / A_1. The Ohio Department of Highway (1947) conducted test of concrete pile caps supported by a single H-pile by direct contact and found that that failure of the steel section can occur before the concrete cap fails. Tests with area ratios (A_2 / A_1) of 121 resulted in a bearing strength ratio f_b / f'_c of more than 10. GAI Consultants (1982) conducted full-scale pile cap tests with multiple H-piles to investigate the influence of flexural action on the bearing strength of concrete. They reported a bearing strength ratio of 8 ($f_b / f'_c = 8$) given that adequate pile embedment and edge distance were provided.

The elimination of the bearing plate improves the practicality of placement of sound concrete around the embedded ends of micropiles and aids in achieving better concrete density in those regions near the top of the micropiles. It also improves the integrity of the concrete pile cap by eliminating potential large surface cracks in the relatively small cap, because of the high lateral-stress-induced de-bonding between the smooth steel plates and surrounding concrete. It reduces the construction cost and time as well.

EXPERIMENTAL TEST SETUP DESCRIPTION

A full-scale micropile cap supported by two micropiles was designed, constructed, and tested to 2.33 times the design load. The micropiles consisted of HSS steel casing filled with grout. The outside diameter of the HSS casing was *194* mm (*7.625* inch) with a wall thickness *11* mm (*0.43* inch). The specified yield stress of the steel casing was *550* MPa (*80* ksi), and the specified compressive strength of the cement grout was *50* MPa (*7250* psi).

The loading apparatus consisted of two crossed reaction beams held by four tie-

downs at each end of the reaction beams as shown in Figure 1. The axial load was applied to the micropile cap by a hydraulic jack installed between the micropile cap and the reaction beams.

The test micropile cap was cast monolithically with two micropile heads having *152* mm (*6* inch) embedment. No bearing plates were installed. The geometry of the cap was *1803*mm (71 in) x *1016* (40 in) x *1219* (48 in) as shown in Figure 2. The spacing between the micropiles was 787 mm (31 in). The cap was reinforced with *6*-25M rebars of total area *3000* mm^2 (*4.65* in^2) in the longitudinal direction and *10*-25M rebars of total area *5000* mm^2 (*7.75* in^2) in the transverse direction. The jacking load was applied to a *63.5* mm (2.5 in) thick by *610x610* mm (24 in x 24 in) steel plate grouting to the centre of the cap top.

The load increments and total load applied to the micropile cap were measured with a jack pressure dial. Four electrical-resistance strain gages were installed at mid-spans of the 4 central longitudinal rebars. These strain gages were used to record the strain level in the longitudinal reinforcement (behaving as ties in the strut-and-tie model).

To eliminate the influence of the potential vertical soil reaction on the micropile cap, a 102 mm (*4* inch) gap was left underneath the pile cap. Backfill soil surrounding the pile cap was compacted to provide restraint against lateral movement.

Due to the test apparatus capacity, the specified concrete compressive strength was *30* MPa (*4350* psi) to ensure the bearing splitting failure could be achieved. Four 150 mm x 600 mm (3 in x 6 in) concrete cylinders were embedded in each top corners of the pile cap. The concrete samples were testing within days of the test day to verify actual concrete strength. Results from laboratory compressive tests of the four cylinders were *25.9* MPa, *34.3* MPa, *38.4* MPa, and *38.9* MPa.

The jacking load on the micropile cap was cycled in 25% increments of design load to failure. The strains in the reinforcement, casing, and concrete and the movement of the pile cap were collected via a data logger and manual recording.

FINITE ELEMENT MODEL

The micropile cap was modeled with the finite element analysis FEA code, DIANA (Release 9). A quarter of the three dimensional finite element mesh of the micropile cap is shown in Figure 3. The elements used to model concrete, grout, and steel consisted of twenty-node isoparametric. Eight by eight (8x8) three dimensional interface elements were chosen for the interface between the concrete, steel and grout. A 3x3x3 Gaussian integration scheme for the solid elements and a 3x3 Gaussian integration scheme for the interface elements were adopted. Twenty-node isoparametric solid brick elements improve convergence, prevent potential shear and volumetric locking, and eliminate the potential spurious zero-energy deformation modes. For consistency, the interface elements were also chosen from the higher order elements.

Figure 1. Picture of Test setup

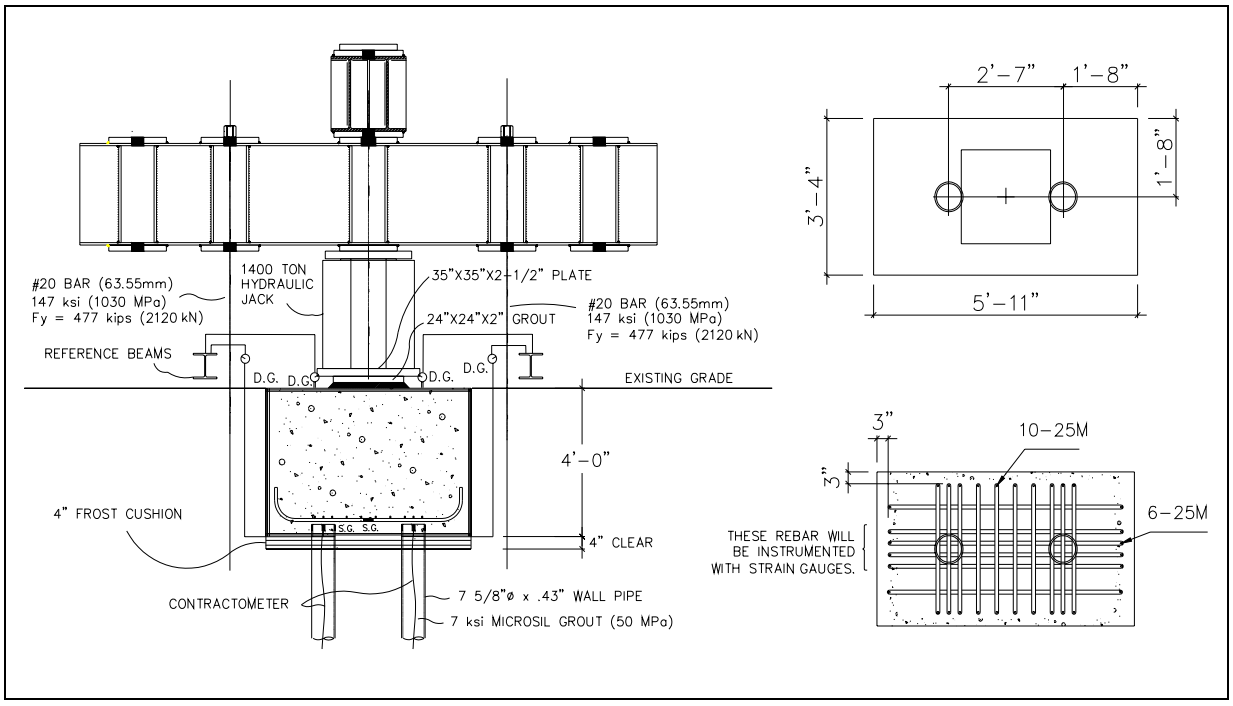

Figure 2. Plan view and section of micropile cap test setup

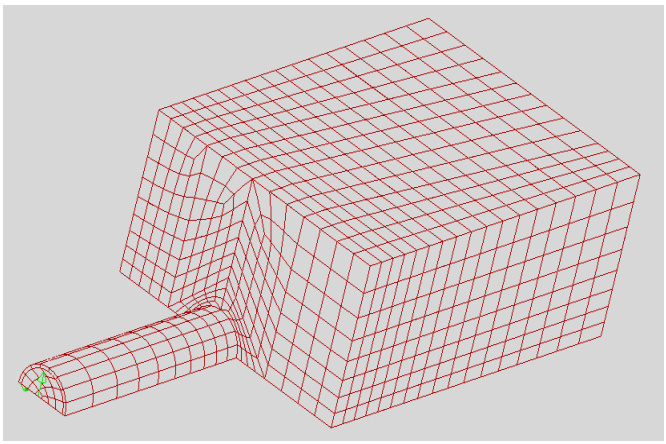

Figure 3. FE mesh of one quarter model

The Modified Maekawa concrete model (TNO DIANA, 2005) was chosen as the concrete material model in the FE analysis for the pile cap. It combines the advantages of the Maekawa model (Maekawa, et al, 2003) in simulating the crushing in the compressive regime and the so-called total-strain based model for the tensile regime. The attractive points of the Modified Maekawa concrete model are that (1) it is formulated based on the multi-axial damage plasticity theory; (2) it has the capability to handle non-orthogonal multi-directional cracking, which is widely known to be robust for crack representation; (3) it checks the unloading/reloading in the total strain directions; and (4) it includes the compression and shear non-linearity.

The embedded reinforcing steel bars with standard hooks are treated in the smeared manner in the FE model, i.e., uniformly distributed over the predefined reinforcement grid plane, and uniformly distributed into the crossed concrete elements. The standard elasto-plastic approach is used to describe the behavior of the reinforcing bar material.

The discontinuities between the concrete of the pile cap, casings and grout of the micropiles are assumed to be governed by a Coulomb friction behavior. The friction coefficient for the steel casing and concrete of the cap is *0.25*, and *0.6* for the grout of the micropiles and concrete of the cap. The cohesion between the grout and concrete is assumed to be half of the concrete tensile strength.

The computation was performed by incremental loading, with sufficient iterations in each increment to achieve equilibrium. The Quasi-Newton method is adopted for the iteration, which essentially uses the information of previous solution vectors and out-of-balance force vectors during the increment to achieve a better approximation. The line-search algorithm was used to accelerate the iteration convergence. Arc-length control algorithm was adopted to render the post-cracking behavior of concrete.

COMPARISON OF LOAD TESTS RESULTS AND PREDICTIONS

The structural capacity of the pile cap was *220%* of the design load, which is *7594* kN (*1707* kip). A class A analysis was performed and where the ultimate capacity of the micropile cap was predicted to be *7740* kN (*1740* kip). The micropile cap actually failed at the load of 8048 kN (*1808* kip) after maintaining the load for about *20* minutes. The predicted load capacity and the test result were within 4%.

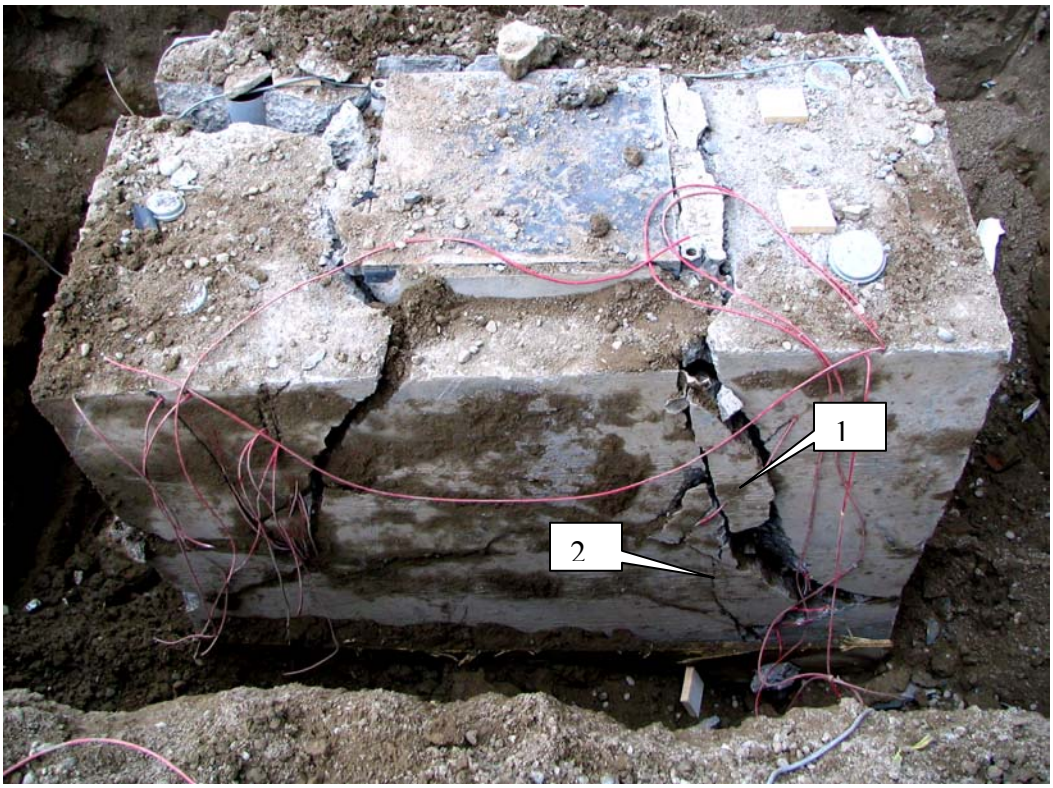

Figure 5. Longitudinal Face of Pile Cap after Failure

The actual cracking pattern at failure of the micropile cap is shown in Figures 5 and 6. Inspection of the cracking pattern suggests that the pile cap failed in bearing as anticipated. There was neither apparent vertical flexural cracking, nor diagonal convex cracking in the shear regions between the two inner sides of the micropiles and the loading edges.

On the longitudinal side face, the cracks were formed in a splitting way with many crossed and scattered cracks. The main cracks were formed either almost in a straight line extending from the centerlines of the micropiles to the loading edge (see #1 in figure 5), or in a concave curve representing a splitting and spalling of concrete (see #2 in figure 5). On the transverse side face, the main crack was almost in a straight vertical line (see #3 in figure 6), accompanied by many crossed horizontal cracks (see #4 in figure 6). This is typical bursting cracking pattern in concrete bearing failures.

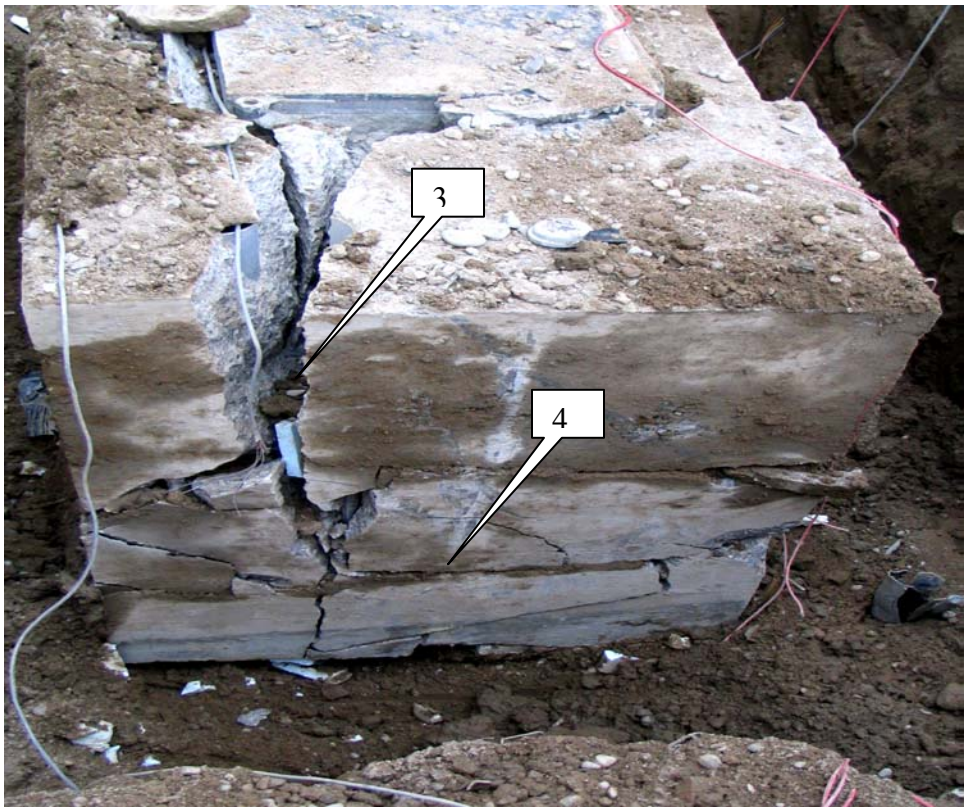

Figure 6. Transverse Face of Pile Cap after Failure

The compressive stress levels in the pile cap concrete of the quarter model are depicted in figure 7. This figure shows the stresses in psi. The double lines near the top of the micropile depict the layer where the rebar is modeled. The concrete strut in a convex arch shape is formed to transfer the applied load from the top plate to the micropiles. It is not a straight strut as assumed in the strut-and-tie mechanism which is adopted in the pile cap design for flexure. In figure 8 it can be seen that the bearing stresses are not uniformly distributed along the top of the micropile.

The cracking pattern of the quarter model of the analytical solution is demonstrated in figure 9. The actual cracking pattern, shown in figure 3, and the predicted cracking pattern, shown in figure 9 are very similar. The FEM is capable of capturing the bearing splitting behavior of the micropile cap and simulate the post-cracking behavior after the pile cap strength is reached.

The predicted and actual stress level in the reinforcing bars at mid-span of the pile cap versus the applied load levels are presented in Fig. 10. One main finding is that the rebar is in compression rather than tension mid span of the pile cap. A possible explanation for this phenomenon is that the concrete beneath the compressive arch strut provides adequate tensile stress to hold the struts. Furthermore, the compression stress in the central longitudinal reinforcement partially balances the tensile stress in the concrete and reinforcement outside the central region, which is produced primarily by the concrete splitting action in the concrete.

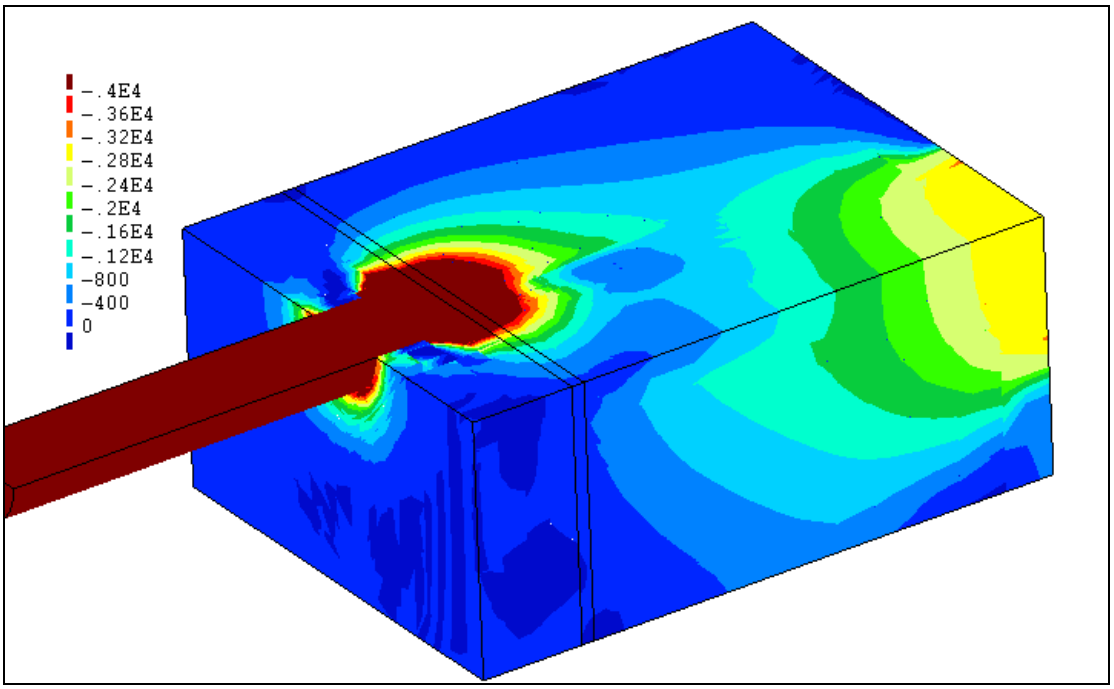

Figure 7. Compressive strut of concrete

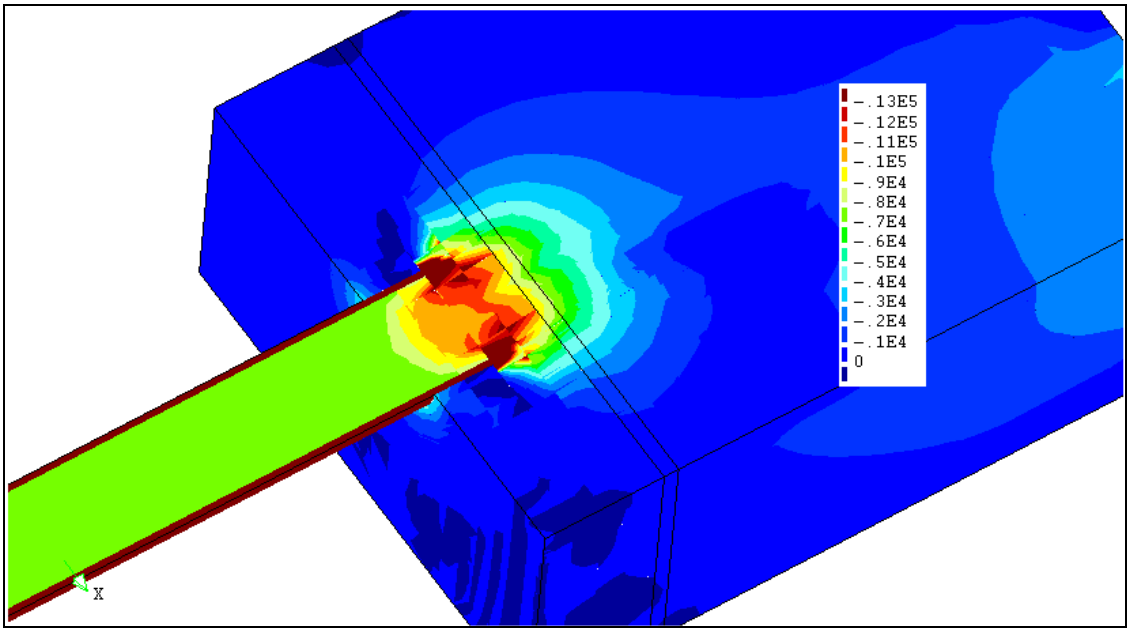

Figure 8. Bearing stress in concrete

The results of the FEA show the stress level in the reinforcing steel is close to the measured stresses as recorded in the rebar strain gauges. This indicates that the smeared treatment of the reinforcing steel over the grid plane and the crossed elements is appropriate for the FE modeling with compatible deformation between concrete and reinforcing steel.

The experimental and analytical results shown in Fig. 8 indicate the reinforcing steel at mid-span is only lightly stressed.

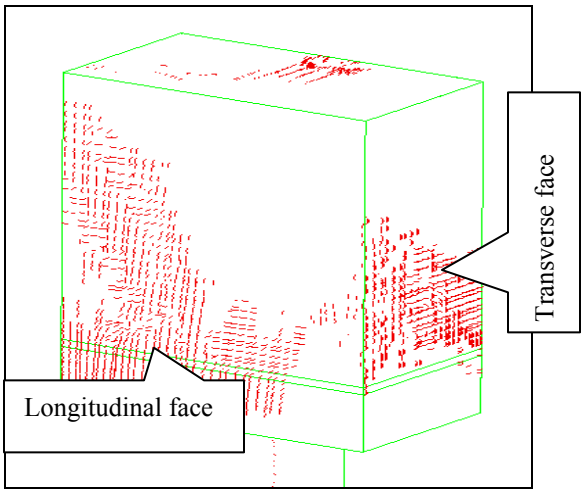

Figure 9. Cracking pattern

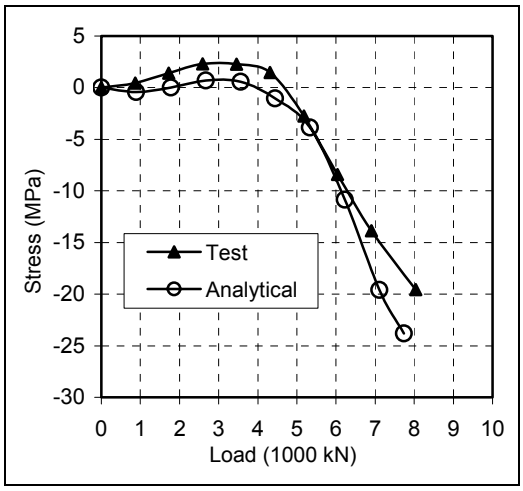

Figure 10. Rebar stress – load level

Figure 11 shows a plan view of the longitudinal stresses along where the rebar has been modeled. Only one quarter of this plan is shown due to symmetry. This is just before the pile cap fails. The stress in the central mid-span region is negative, confirming that the reinforcing bars are in compression. The strut-and-tie model seems to fail in this region. The longitudinal stress distribution in the reinforcement is localized.

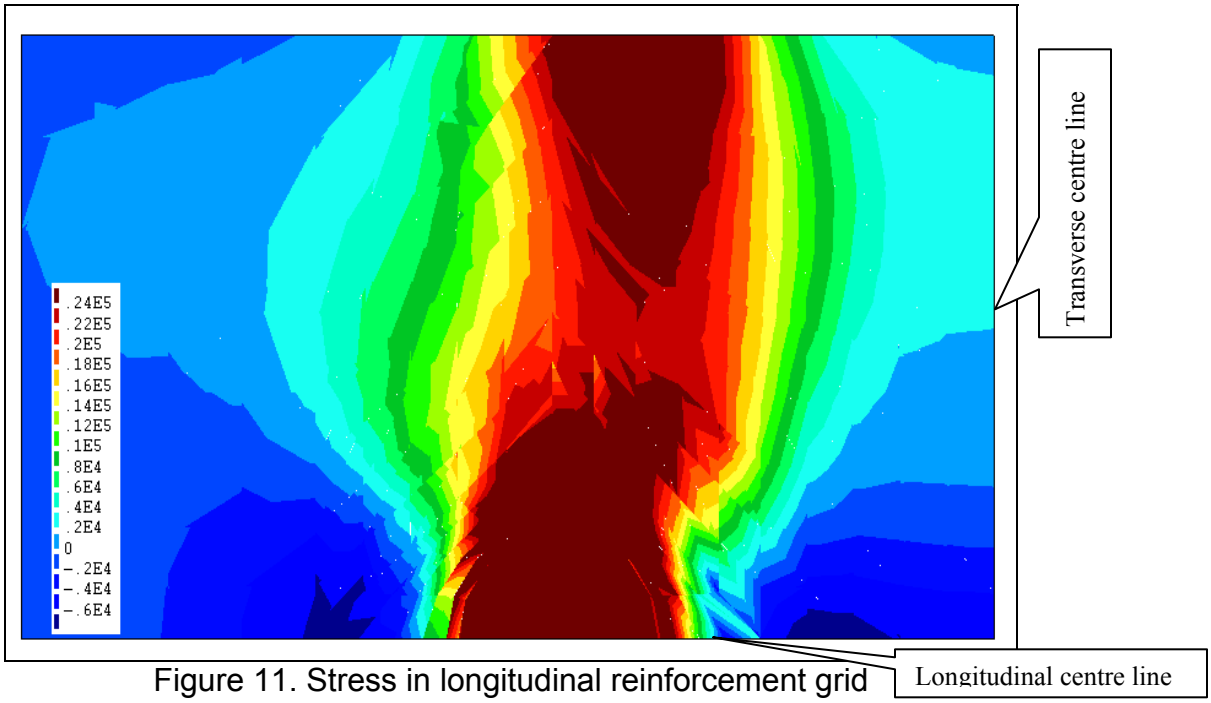

Figure 11. Stress in longitudinal reinforcement grid

CONCLUSIONS

A full-scale micropile cap testing was carried out to failure. No plates above the micropiles were used. A class A analysis using FEA was used to further understand the stress distribution in the pile cap. The analytical results for the ultimate load capacity, the cracking pattern, and the stress level of the reinforcing bars agree well with the experimental results.

Assuming the load was equally divided among both micropiles and the load was supported by the top of the micropile only the average bearing stress was on top of each micropile was 136 MPa (*19.8* ksi) This stress represents *4.5* times the specified concrete compressive strength and *4.0* times the average tested concrete strength. The bearing strength ratio is much higher than the predictions provided by existing concrete design codes such as the value of *1.7* from the ACI code. An extended research and revision of the bearing strength of concrete seems to be necessary in order to achieve more reasonable results.

If bearing failure is a concern, uniform distribution of reinforcing ties over above the micropiles is preferred. The uniform distribution of steel also enables the steel to yield progressively under the bending stress, achieving a favorite ductile behavior of the micropile cap. Additional closed lateral steel hoops along the extensions of the 90 degree standard hooks within the height of highly stressed bearing regions can be used to achieve additional confinement and better structural performance both in load capacity and ductility.

It is concluded that the ultimate load of 8048 kN (*1808* kip) corresponded to a bearing limit state. It is believed that concrete confinement is the critical mechanism to significantly contribute to the load capacity of the pile cap. Although many researchers have made many advances on the issue of concrete bearing strength, the mechanism of the bearing failure of concrete with lateral concrete and reinforcement confinement is still not well understood due to its complexity and, therefore, much remains to be done. From the experimental and analytical results agree that steel bearing plates are not necessary in this application.

ACKNOWLEDGEMENT

The research and experiment work in this paper was partly funded by Geo-Foundations Contractors Inc. The authors wish to express their appreciation to Jim Bruce, P.Eng, for his support of this valuable research.

REFERENCES

ACI 446.1R-91: “Fracture Mechanics of Concrete: Concepts, Models and Determination of Material Properties,” reported by ACI Committee 446, 1999.

ACI 446.3R-97: “Finite Element Analysis of Fracture in Concrete Structures: State-of-the-Art,” reported by ACI Committee 446, 1997.

Adebar, P. and Zhou, Z., “Bearing Strength of Compressive Struts Confined by Plain Concrete,” *ACI Structural Journal*, Vol. 90, No. 5, Sept.-Oct. 1993, pp. 534541.

CEB-FIP, *CEB-FIP Model Code 1990*, Comite Euro-International du Beton, 1993.

GAI Consultants, Inc., “The Steel Pile - Pile Cap Connection,” American Iron and Steel Institute, August 1982.

Hawkins, Neil M., “Bearing Strength of Concrete Loaded through rigid plates,” *Magazine of Concrete Research* (London), Vol. 20, No. 62, March 1968, pp. 31-40.

Hsieh, S. S., Ting, E. C., and Chen, W. F., “A plasticity-Fracture Model for Concrete,” *International Journal of Solids and Structures*, Vol. 18, No. 3, 1982, pp. 181-197.

Komendant, A. E., *Prestressed Concrete Structures*, McGrow-Hill, New York, 1952, pp.172-173.

Marti, P., “Size Effect in Double-Punch Tests on Concrete Cylinders,” *ACI Materials Journal*, Vol. 86, No. 6, Nov.-Dec. 1989, pp. 597-601.

Maekawa, K, Pimanmas, A., and Okamura, H., *Nonlinear Mechanics of Reinforced Concrete*, Spon Press, London, 2003.

Niyogi, S. K., “Bearing Strength of concrete – Geometric Variations,” *ASCE Journal of the Structural Division*, Vol. 99, N0. ST7, July 1973, pp. 1471-1490.

Niyogi, S. K., “Bearing Strength of concrete – Support, Mix, Size Effect,” *ASCE Journal of the Structural Division*, Vol. 100, N0. ST8, July 1974, pp. 1685-1702.

Ohio Highway Department, “Investigation of the Strength of the Connection between A Concrete Cap and the Embedded End of A Steel H-Pile,” Research Report No. 1, State of Ohio, Dec. 1947.

TNO DIANA, Material Library, User’s manual, April 2005.